Toxicology and Applied Pharmacology 341 (2018) 38–50

Contents lists available at ScienceDirect

Toxicology and Applied Pharmacology

journal homepage: www.elsevier.com/locate/taap

Pinocembrin from *Penthorum chinense* Pursh suppresses hepatic stellate cells activation through a unified SIRT3-TGF-β-Smad signaling pathway

Fayang Zhou, Anqi Wang, Dan Li, Yitao Wang, Ligen Lin*

State Key Laboratory of Quality Research in Chinese Medicine, Institute of Chinese Medical Sciences, University of Macau, Macao, China

ARTICLE INFO

Keywords:
Liver fibrosis
Hepatic stellate cells
Penthorum chinense Pursh
Pinocembrin
Sma- and Mad-related proteins
Silent mating type information regulation 2 homolog 3

ABSTRACT

The inactivation of hepatic stellate cells (HSCs) has been verified to be an effective therapeutic strategy for treatment of liver fibrosis. *Penthorum chinense* Pursh has been widely used to protect liver in China; while, the role of *P. chinense* Pursh in treatment of liver fibrosis is still unexplored. In the current study, the aqueous extract of *P. chinense* Pursh (PCE) was found to suppress the expressions of fibrotic markers, including collagen I and α-smooth muscle actin (α-SMA), in human HSCs (LX-2); and its major active constituent, pinocembrin (PIN), was discovered to inhibit the expressions of fibrotic markers in LX-2 cells and rat HSCs (HSC-T6). Further study indicated that PIN suppressed the activation of LX-2 and HSC-T6 cells through elevating the expression and activity of silent mating type information regulation 2 homolog 3 (SIRT3). *Via* SIRT3, PIN activated superoxide dismutase 2 (SOD2), to alleviate the accumulation of reactive oxygen species (ROS) and inhibit phosphoinositide 3-kinase (PI3K)-protein kinase B (Akt) signaling, resulting in decreased production of transforming growth factor-β (TGF-β) and nuclear translocation of the transcription factor Sma- and Mad-related proteins (Smad). Furthermore, PIN activated glycogen synthase kinase 3β (GSK3β) through SIRT3, to enhance Smad protein degradation. Taken together, PCE and PIN were identified as potential anti-fibrotic agents, which might be well developed as a candidate for treatment of liver fibrosis.

1. Introduction

Fibrotic diseases account for up to 45% of deaths in the developed countries (Pellicoro et al., 2014). Liver fibrosis is a wound-healing response characterized by the accumulation of extracellular matrix (ECM) following either acute or chronic liver injury (Hernandez-Gea and Friedman, 2011). Liver fibrosis results in the deformation of normal liver architecture, and ultimately can be aggravated and developed into liver cirrhosis and even to hepatocellular carcinoma (Affo et al., 2017). However, effective anti-fibrotic therapies are still lacking.

Substantial evidences have recognized activation of hepatic stellate cells (HSCs) plays a key role in liver fibrosis (Troeger et al., 2012; Puche et al., 2013; Yin et al., 2013). Activated HSCs undergo transdifferentiation to fibrogenic myofibroblast-like cells, resulting the production of collagen I and other ECM components (Inagaki and Okazaki, 2007). Activated HSCs also exhibit characteristic of contractile cells that highly express the cytoskeletal protein α-smooth muscle actin (α-SMA) (Shi and Rockey, 2010).

Transforming growth factor-β (TGF-β) is a multifunctional cytokine that plays an important role in growth, development, inflammation and host immunity (Massague, 2012). Among three different isoforms, TGF-β1 is established as the master regulator of fibrosis (Meng et al., 2016). Hitherto the regulation of TGF-β1 is still blurring. However, evidences have indicated that reactive oxygen species (ROS)-mediated Akt phosphorylation is essential for the production of TGF-β1 (Remy et al., 2004; Zhang et al., 2013; Suzuki et al., 2014). Once produced, TGF-β1 acts through canonical Smad signaling pathway (Schmierer and Hill, 2007; Zhang, 2009). Generally, the receptor-regulated Smads (r-Smad), typically Smad2/3, are phosphorylated at specific modification sites to activate, and subsequently bind to the common-mediator Smad (co-Smad) or other related transcription factors (Macias et al., 2015; Meng et al., 2016). Through this process Smad complexes are enabled to translocate to the nucleus and transcribe specific genes (Massague et al., 2005).

Sirtuins are NAD^+-dependent protein deacetylases that include seven isoforms in mammalian cells (Houtkooper et al., 2012). As a longevity protein, SIRT3 is primarily localized in mitochondria and widely reported to regulate mitochondrial function, cell survival, and organismal aging through deacetylating specific proteins (Hirschey et al., 2010; Someya et al., 2010; Hebert et al., 2013). SIRT3 directly deacetylates isocitrate dehydrogenase 2 (IDH2) and superoxide dismutase 2 (SOD2) to augment anti-oxidative capacity (Qiu et al., 2010;

* Corresponding author.
E-mail address: ligenl@umac.mo (L. Lin).

https://doi.org/10.1016/j.taap.2018.01.009
Received 17 October 2017; Received in revised form 3 January 2018; Accepted 13 January 2018
Available online 02 February 2018
0041-008X/

Yu et al., 2012). SIRT3 also deacetylates and activates glycogen synthase kinase 3β (GSK-3β) to positively regulate its activity, which contributes in the phosphorylation of β-catenin and Smad, and thereby blocks TGF-β1 signaling and tissue fibrosis (Sundaresan et al., 2016). Since SIRT3 plays a key role in regulating anti-oxidative capacity and fibrogenesis, it is considered to be a promising therapeutic target for prevention and treatment of liver fibrosis.

Penthorum chinense Pursh (Penthoraceae), is widely distributed in China. In the region of Miao nationality, the water decoction of this plant has been used for thousands of years to protect liver from alcoholic injury. The *P. chinense* decoction is involved in many food or health products used for liver protection in China. Previous studies have disclosed *P. chinense* extracts possess protective effect against hepatitis B, hepatitis C, hepatocarcinoma (Wang et al., 2015), and ethanol- or oxidant-induced liver injury (Cao et al., 2015; Hu et al., 2015; Wang et al., 2016). Tens of flavonoids, lignans and steroids were identified from this plant with anti-oxidative, anti-carcinomatous, and hypoglycemic effects (Lu et al., 2012; Zeng et al., 2013; Huang et al., 2014; Wang et al., 2014; He et al., 2015a; He et al., 2015b; Huang et al., 2015). Although many chemical and pharmacological studies have been carried out on *P. chinense* (Wang et al., 2015), the anti-fibrotic effect is remaining unknown. In the current study, we attempt to investigate the water extract of *P. chinense* and its major bioactive compound in suppressing HSCs activation in human immortalized LX-2 and rat immortalized HSC-T6 cells. Additionally, we intend to elucidate whether the anti-fibrotic effect of *P. chinense* is through SIRT3-TGF-β-Smad signaling pathway.

2. Materials and methods

2.1. Chemicals and reagents

Phosphate buffered saline (PBS) powder, Dulbecco's Modified Eagle's medium (DMEM), P/S solution (Penicillin 10,000 U/ml, Streptomycin 10,000 μg/ml), 0.25% (w/v) trypsin/1 mM EDTA, and fetal bovine serum (FBS) were purchased from Gibco (Waltham, MA, USA). 3-(4,5-dimethylthiazolyl-2)-2,5-diphenyltetrazolium bromide (MTT), dichloro-dihydro-fluorescein diacetate (DCFH-DA), paraformaldehyde (PFA), Hoechst 33342, MK2206, SC79, AGK7, and SB216763 were purchased from Sigma-Aldrich (St. Louis, MO, USA). RIPA lysis buffer was purchased from Beyotime Biotechnology Company (Shanghai, China). Protein A/G agarose and *SIRT3* shRNA plasmid were purchased from Santa Cruz Biotechnology (Santa Cruz, CA, USA). Pierce BCA assay kit, NE-PER Nuclear and Cytoplasmic Extraction Reagents kit, Goat anti-Rabbit IgG secondary antibody, West Femto Sensitivity Substrate, and Lipofectamine 2000 were purchased from Thermo Fisher Scientific (Waltham, MA, USA). Primary antibodies of collagen I, α-SMA, and β-actin were obtained from Abcam (Cambridge, UK). All other primary and secondary antibodies were purchased from Cell Signaling Technology (Danvers, MA, USA). Enzyme linked immunosorbent assay (ELISA) kit for determination of α-SMA and TGF-β1 content in medium were purchased from Shanghai Yaoyun Chemistry Biological Technology Co., Ltd. (Shanghai, China) and NeoBioscience Technology Co., Ltd. (Shenzhen, China), respectively. Pinocembrin (PIN, ≥ 98%) was separated from *P. chinense* previously (Wang et al., 2016).

2.2. Cell culture

Human immortalized HSCs LX-2 cells and rat immortalized HSCs HSC-T6 cells were gifts from Professor S. L. Friedman (Liver Disease Research Center of San Francisco General Hospital, CA, USA). The cells were cultured in DMEM supplemented with 10% FBS and 1% P/S in a 5% CO_2 atmosphere at 37 °C. Cells were seeded onto applicable tissue culture dishes or plates at 70–80% confluence for the following experiments.

2.3. Cell viability assay

LX-2 or HSC-T6 cells were seeded onto 96-well plates at a density of 1×10^4 cells per well. When approximately 70–80% confluence, cells were treated with or without different concentrations of designated compounds for 24 h. Subsequently, cell viability was determined by incubation with DMEM containing MTT (1 mg/ml) for 4 h, followed by dissolving the formazan crystals with DMSO. The absorbance at 570 nm was measured by a FlexStation 3 Multi-Mode Microplate Reader (Molecular Devices, California, USA). The results were analyzed based on at least three independent experiments.

2.4. Generation of SIRT3 knockdown cell line

LX-2 cells were cultured in 6-well plate and incubated with antibiotics free medium for 24 h. shRNA targeting *SIRT3* and empty vector were transfected to cells using Lipofectamine 2000, following the manufacturer's instruction. Six hours after transfection, medium was changed to fresh culture medium. Forty-eight hours after transfection, 10 μg/ml puromycin was added to the medium to select positive cells for 14 days. Medium was changed every other day. The positive cells were pooled together.

2.5. Measurement of extracellular α-SMA and TGF-β1

To measure α-SMA and TGF-β1 content in medium, LX-2 cells were seeded onto 96-well plates at a density of 5×10^3 cells/well. When reaching approximately 70–80% confluence, cells were treated with or without different concentrations of indicated compounds for 24 h. Then culture medium was collected for determination of α-SMA and TGF-β1 content through ELISA assays according to the manufacturer's instructions.

2.6. ROS determination

A fluorescent probe, DCFH-DA, was used for determination of intracellular ROS levels. LX-2 cells were seeded onto 96-well black plates at a density of 5×10^3 cells/well for 24 h. Cells were pretreated with or without different concentrations of concrete compounds for 24 h. Then cells were washed with PBS for three times and incubated with DCFH-DA (10 μM) at 37 °C for 15 min. Subsequently, cells were washed with PBS for three times and the intracellular fluorescent intensity was determined by a FlexStation 3 Multi-Mode Microplate Reader with the excitation and emission wave lengths at 485 and 535 nm, respectively. Meanwhile, an Incell Analyzer 2000 was used to observe the intracellular fluorescence. Results were presented as relative fluorescent intensity based on at least three independent experiments.

2.7. Immunofluorescent assay

LX-2 cells were plated on glass coverslips in dish grown to about 50% confluence and then treated with or without definite compounds for 24 h. Subsequently, cells were washed twice in PBS and fixed with 4% (v/v) PFA in PBS for 1 h at room temperature. Cells were then rinsed twice with PBS and permeabilized with 0.1% Triton X-100 in PBS for 1 h. After rinsing with PBS, cells were blocked with PBS supplemented with 5% (w/v) BSA for 1 h. Thereafter, incubated with anti-collagen I, anti-α-SMA, anti-Smad3 or anti-β-catenin antibody overnight at 4 °C. Cells were washed three times in PBS and then incubated for 1 h at room temperature with Texas red- or Alexa Fluor 488-conjugated secondary antibody. Cells were then rinsed three times in PBS and the nuclei were counterstained with Hoechst 33,342 for 5 min at room temperature. Observation of the intracellular fluorescence was performed on a Leica TCS SP8 Confocal Laser Scanning Microscope System.

2.8. Western blotting

LX-2 or HSC-T6 cells grown on 10 cm tissue culture dishes were treated with or without different concentrations of indicated compounds for 24 h, and then the cells were harvested by treating with ice-cold RIPA lysis buffer containing PMSF and protease inhibitor cocktail (100:1:1, v/v/v). After vortexed thoroughly, the cell debris was removed by centrifugation at 16,000 *g* for 30 min and the supernatant was collected for protein concentration determination using the Pierce BCA assay kit according to the manufacturer's instructions. Subsequently, the same amount of proteins was separated by sodium dodecyl sulfate polyacrylamide gel electrophoresis (SDS-PAGE), transferred to polyvinylidene difluoride (PVDF) membranes, and then blocked with 5% non-fat milk in TBST buffer (100 mM NaCl, 10 mM Tris-HCl, pH 7.5 and 0.1% Tween-20) for 1 h at room temperature. Then, membranes were incubated with primary antibodies in TBST buffer overnight at 4 °C with shaking. After washing with TBST buffer for three times, a secondary HRP-linked antibody was added and incubated at room temperature for 4 h, followed by washing in TBST wash buffer for another three times. Then the membranes were incubated with West Femto Sensitivity Substrate and protein bands were detected using a ChemiDoc XRS Molecular Imager system (Bio-Rad, California, USA). All the western blotting quantifications were conducted on Image Lab (Bio-Rad, California, USA).

2.9. Nucleocytoplasmic fractionation

Nucleocytoplasmic fractionation was conducted using the NE-PER Nuclear and Cytoplasmic Extraction Reagents kit according to the manufacturer's protocol. In brief, cells were harvested with trypsin-EDTA and then washed three times with ice-cold PBS prior to fractionation. Then, appropriate volume of Cytoplasmic Extraction Reagent I (CER I) containing PMSF and protease inhibitor cocktail (100:1:1, v/v/v) was added to the cell pellet. After vortex and incubation on ice for 10 min, CER II was added to each tube, followed by vortex and incubating on ice for 1 min. After centrifuging at 16,000 *g* for 5 min, the supernatant was collected as cytoplasmic fraction. The insoluble pellet containing nuclear fraction was suspended in ice-cold Nuclear Extraction Reagent (NER) containing PMSF and protease inhibitor cocktail (100:1:1, v/v/v). After vortexed, the solution was centrifuged at 16,000 *g* for 10 min, to collect the supernatant as nuclear fraction. Protein concentrations of cytosol and nuclear fractions were determined with BCA kit. Samples were prepared for subsequent western blot analysis.

2.10. Immunoprecipitation

To examine the acetylation level of SOD2 and GSK-3β, the IP/Western blot analysis were performed. The detailed procedure was described as following: protein A/G agarose beads were washed with RIPA lysis buffer for three times prior to immunoprecipitation. Primary SOD2 or GSK-3β antibody was incubated with protein A/G agarose beads at 4 °C for 1 h with gently mixing. Next, cellular protein samples were extracted and incubated with the antibody-bead mixture at 4 °C under rotary agitation overnight. The immune complex was washed by ice-cold RIPA lysis buffer for three times and boiled in protein loading buffer for 10 min at 95 °C. Finally, the immunoprecipitate was analyzed by Western blotting.

2.11. Preparation and HPLC-UV analysis of aqueous extract from P. chinense

The aqueous extract of *P. chinense* was kindly gifted by Neautus Traditional Chinese Medicine Co. (Sichuan, China). The preparation procedure was described previously (Wang et al., 2016). In brief, the air-dried whole grass of *P. chinense* was ground into powder and extracted with boiling water for three times, each 5 h. After evaporation of the collected decoction to small volume, alcohol was added in till 60% to precipitate proteins and polysaccharides. Then the supernatant was collected and condensed to yield the aqueous extract. The accurately weighed extract was dissolved in methanol-water (1:1) solution and sonicated for 1 h. After filtered by 0.45 μm Millipore membrane, 20 μl filtration was injected into an Agilent SB C18 column (250 × 4.6 mm, 5 μm), which was maintained at 35 °C for gradient elution with 0.1% aqueous acetic acid (A) and acetonitrile (B). The elution program was set as follows: 0–6 min, 95% A; 6–12 min, 95–85% A; 12–55 min, 85–50% A; 55–60 min, 50–10%. The detection wavelength was set at 254 nm. Representative chromatogram was analyzed using a Waters Empower system (Waters, MA, USA) and the content of PIN and other ingredients (%) in the water extract of *P. chinense* was determined by comparing the peak area with that of standard compounds. The water extract was dissolved by 80% methanol solution at concentration of 3.68 mg/ml, while PIN was dissolved by 60% methanol solution at concentration of 10.25 μg/ml.

2.12. Statistical analysis

The statistical analysis was performed using GraphPad Prism 7.04 (GraphPad Software, California, USA). All values are presented with mean ± SEM. All of the results took at least three biological replicates. The statistical differences between control and experimental groups were determined by one-way ANOVA, with p values < 0.05 considered significant.

3. Results

3.1. Aqueous extract of P. chinense suppressed the expressions of fibrotic markers in hepatic stellate cells

In our previous study, the aqueous extract of *P. chinense* showed potent hepatoprotective effect against *tert*-butyl hydroperoxide (*t*-BHP) induced oxidative injury in L02 cells (Wang et al., 2016). Till now, the role of *P. chinense* in treatment of liver fibrosis is still unexplored. Currently, LX-2 and HSC-T6 cell lines were recruited to evaluate the effect of *P. chinense* aqueous extract (PCE) on suppressing the activation of HSCs *in vitro*.

Firstly, the MTT assay indicated that PCE didn't show obvious cytotoxicity to LX-2 cells when treated with the concentration up to 100 μg/ml for 24 h (Fig. 1A). Moreover, 100 μg/ml PCE did not affect LX-2 cell viability up to 24 h, while showed significant cytotoxicity when prolonging the exposure time to 48 h (Fig. 1B). Thus, LX-2 cells were treated with up to 100 μg/ml PCE for 24 h in the following experiments. The expression of ECMs, including collagen I and α-SMA, were detected in LX-2 cells. The results showed that both collagen I and α-SMA protein levels were decreased by the treatment of PCE in a dose-dependent manner (Fig. 1C). ELISA assay further supported PCE significantly reduced α-SMA secretion in LX-2 cells (Fig. 1D). Regarding HSC-T6 cells, the MTT assay indicated PCE didn't affect cell viability up to 100 μg/ml for 24 h (Fig. S1A). Moreover, prolonged incubation time didn't change the viability of HSC-T6 cells (Fig. S1B). PCE didn't affect the expressions of ECMs in HSC-T6 cells (Fig. S1C).

To further figure out the chemical principles responsible for the suppressing effect of PCE on HSCs activation, thoroughly chemical isolation was performed to identify a series of polyphenols (Table S1). The cytotoxicity of these isolates were listed on Table S2. The inhibitory effect of all isolates on α-SMA secretion was evaluated on LX-2 cells using ELISA assay. The results showed pinocembrin (PIN) was the most effective compound (Fig. 1D). Moreover, pinocembrin-7-*O*-D-glucoside (PING) and 5-methoxy-pinocembrin-7-*O*-D-glucoside (MPING), two PIN glucosides, also significantly decreased α-SMA levels (Fig. 1D). Additionally, kaempferol (KAE) and quercetin (QCT), structural analogues of PIN, were also found to obviously suppress α-SMA level (Fig. 1D).

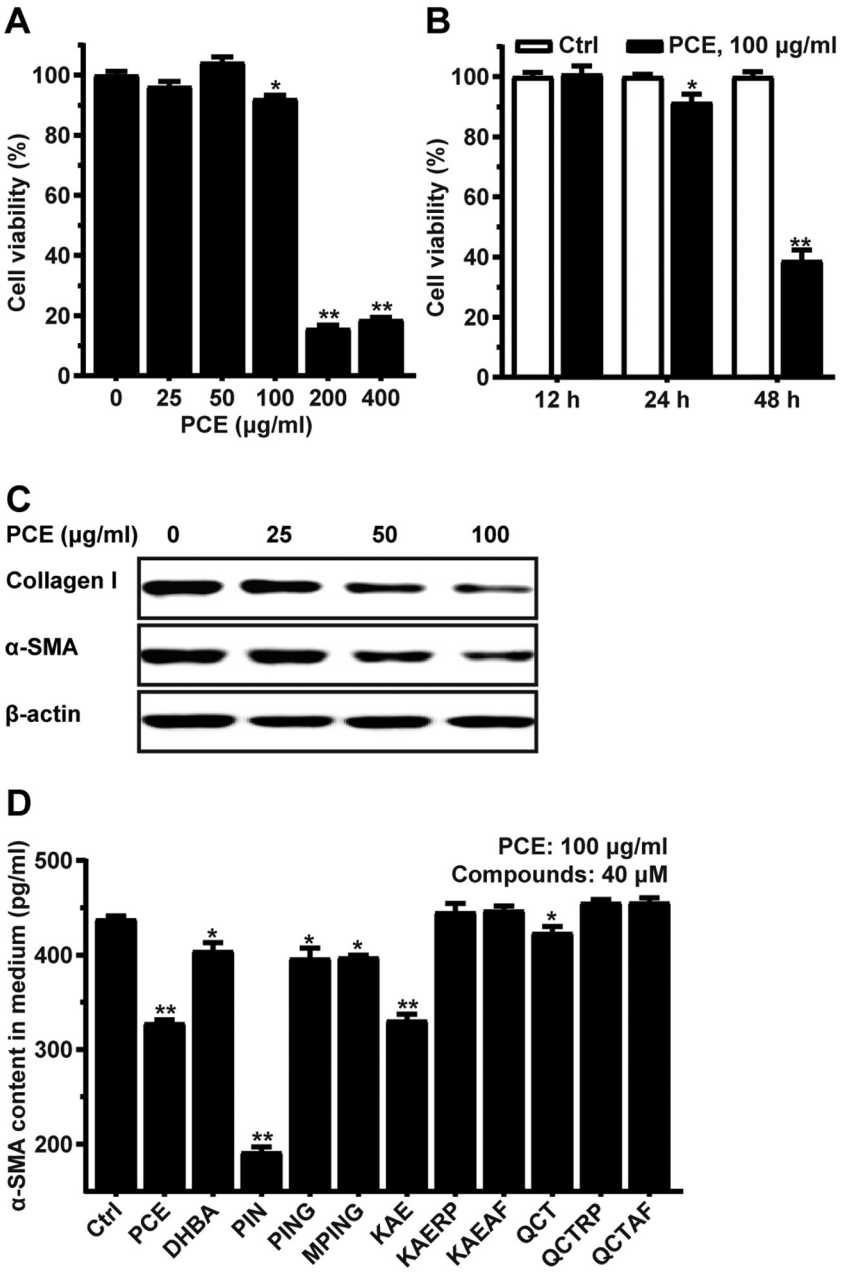

Fig. 1. PCE suppressed the expressions of ECMs in LX-2 cells. The viability of LX-2 cells when treated with different concentrations of PCE for 24 h (A), or 100 μg/ml PCE for different time (B). (C) PCE decreased collagen I and α-SMA expressions in a dose-dependent manner. (D) PCE and isolates suppressed the extracellular secretion of α-SMA. Measurements took $n = 6$ biological replicates. $^{*}p < 0.05$, and $^{**}p < 0.01$ PCE or compound treated group *vs* control group.

However, other isolates, including kaempferol-3-*O*-L-rhamnopyranoside (KAERP) and kaempferol-3-*O*-L-arabinofuranoside (KAEAF), did not show obvious effect on α-SMA secretion (Fig. 1D). Taken together, PCE dose-dependently suppressed the expressions of ECM markers in LX-2 cells, and PIN was identified as the chemical principle for the anti-fibrotic effect of PCE.

3.2. PIN inhibited hepatic stellate cells activation in dose- and time-dependent manners

Since PIN was identified as the most potent compound to inhibit the activation of LX-2 cells, the following experiments was performed on HSCs. Firstly, the MTT assay suggested PIN didn't show obvious cytotoxicity to both LX-2 or HSC-T6 cells up to 40 μM for 24 h (Fig. 2A and B). Prolonged exposure time induced about 15% loss of LX-2 cell viability (Fig. 2C), but didn't affect the viability of HSC-T6 cells (Fig. 2D). Subsequently, the inhibitory effect of PIN on HSCs activation was evaluated. The protein levels of collagen I and α-SMA in both LX-2 and HSC-T6 cells were decreased by PIN treatment in a dose-dependent manner (Fig. 2E). Meanwhile, the expression of these two proteins were down-regulated by PIN with prolonged treatment time (Fig. 2F). The immunostaining images of LX-2 cells also indicated that both collagen I and α-SMA were significantly reduced when treated with 40 μM PIN for 24 h (Fig. 2G and H). Moreover, ELISA assay indicated that the α-SMA content in medium was reduced by PIN treatment in LX-2 cells in a dose-dependent manner (Fig. 2I). The above data suggested that PIN suppressed HSCs activation in dose- and time-dependent manners.

3.3. PIN suppressed hepatic stellate cells activation through inhibiting TGF-β-Smad signaling pathway

TGF-β was well documented as the central mediator in fibrosis (Meng et al., 2016). Intracellular Smad transduced extracellular signals from TGF-β ligands to the nucleus in response to stressors or post translation modifications, and then activated downstream gene transcription (Massague et al., 2005; Schmierer and Hill, 2007; Massague,

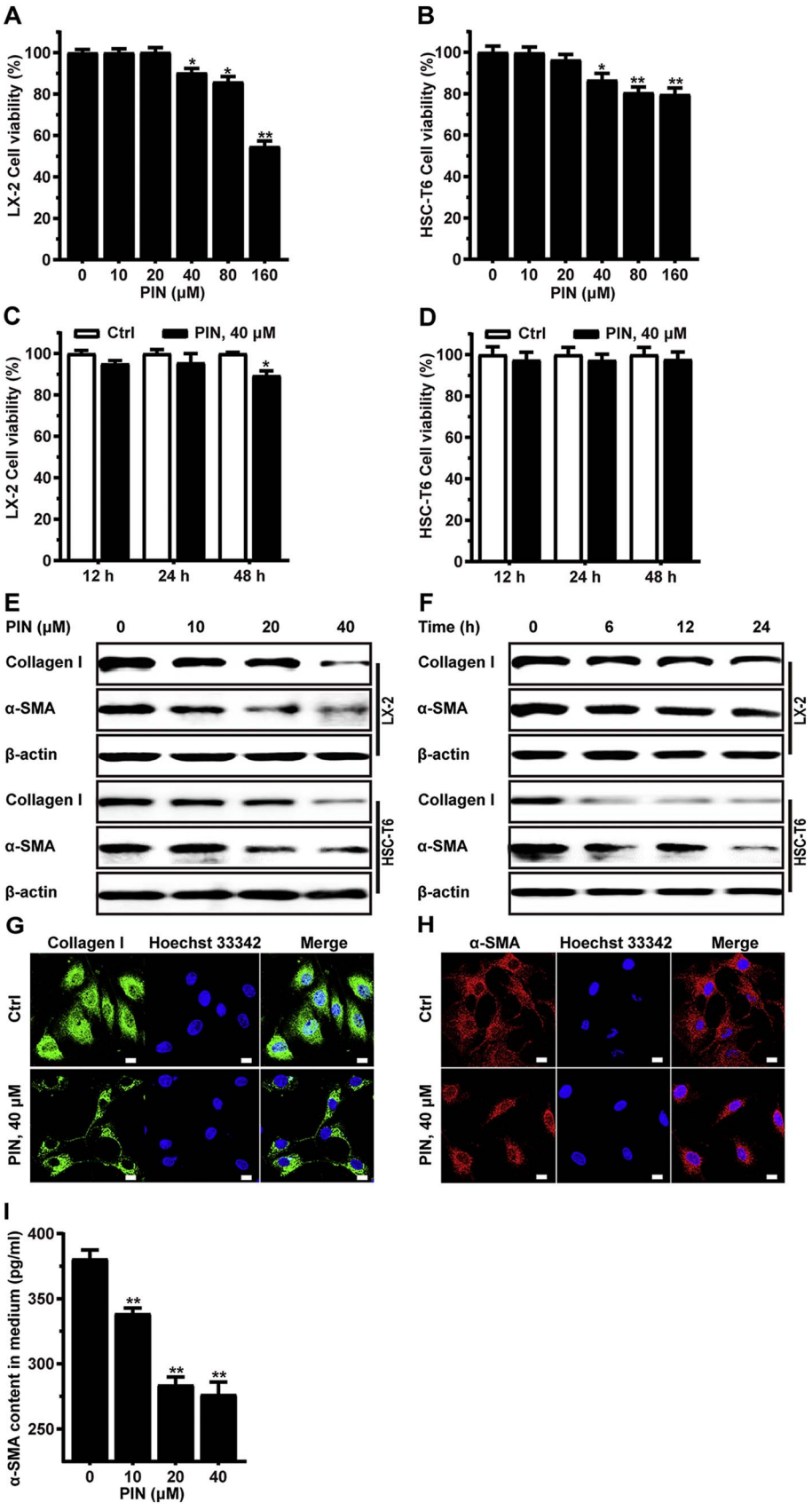

Fig. 2. PIN inhibited HSCs activation. The viability of LX-2 (A and C) and HSC-T6 (B and D) cells when treated with different concentrations of PIN for 24 h, or 40 μM PIN for different time. The expressions of collagen I and α-SMA were evaluated with Western blotting, when treated with different concentrations of PIN for 24 h (E), or 40 μM PIN for different time (F) in LX-2 and HSC-T6 cells. Immunostaining of collagen I (G) and α-SMA (H) were assayed in LX-2 cells treated with 40 μM PIN for 24 h. (I) The extracellular content of α-SMA was determined with ELISA kit. Measurements took $n = 6$ biological replicates, $^{*}p < 0.05$, and $^{**}p < 0.01$ PIN treated group *vs* control group. Scale bar = 12.5 μm.

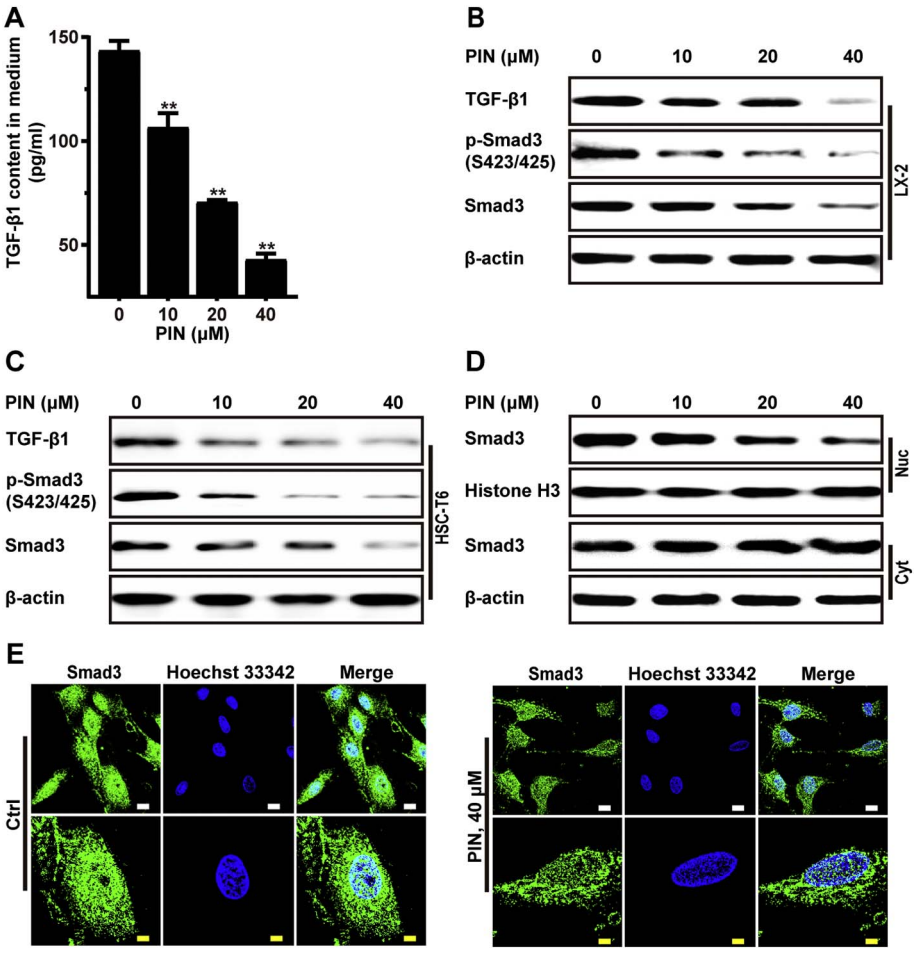

Fig. 3. PIN suppressed HSCs activation through TGF-β-Smad signaling pathway. (A) PIN suppressed the extracellular secretion of TGF-β1 in LX-2 cells in a dose-dependent manner. PIN decreased TGF-β1, total and Ser423/425 phosphorylated Smad3 expressions in LX-2 (B) and HSC-T6 (C) cells. (D) PIN decreased nuclear (Nuc) Smad3 but not cytoplasmic (Cyt) Smad3 protein level in LX-2 cells. (E) Smad3 was excluded from the nucleus in LX-2 cells when treated with 40 μM PIN, assessed by immunostaining. Measurements took $n = 6$ biological replicates. $^{**}p < 0.01$ PIN treated group *vs* control group. Scale bar, 12.5 μm (white) and 5 μm (yellow). (For interpretation of the references to colour in this figure legend, the reader is referred to the web version of this article.)

2012). Thus, we speculated PIN might inhibit HSCs activation though interfering TGF-β-Smad signaling pathway. As expected, the ELISA assay showed the extracellular TGF-β1 was significantly decreased by PIN treatment in LX-2 cells (Fig. 3A). Furthermore, the intracellular TGF-β1 protein in LX-2 cells was lessened by PIN treatment in a dose-dependent manner (Fig. 3B), which was consistent in HSC-T6 cells (Fig. 3C). Next, western blot analysis showed that PIN treatment was associated with decreasing of phosphorylated and total Smad levels in both cells lines (Fig. 3B and C). Further studies indicated that the nuclear Smad was decreased but the cytoplasmic Smad didn't change much when LX-2 cells were exposed with different concentrations of PIN (Fig. 3D). The immunostaining results intuitively indicated that Smad was excluded from the nucleus when treated with PIN (Fig. 3E). All the results indicated that PIN suppressed HSCs activation through reducing TGF-β1 production and secretion, suppressing SMAD phosphorylation and activation, and further blocking its nuclear localization.

3.4. PI3K-Akt signaling was involved in the anti-fibrotic effect of PIN

Inhibition of PI3K-Akt signaling pathway suppressed collagen I synthesis and ECM deposition, and reduced profibrogenic factors (Reif et al., 2003; Son et al., 2013; Wang et al., 2013; Han et al., 2016). As a matter of fact, it was observed that PIN treatment significantly decreased the phosphorylation levels of PI3K and Akt in a dose-dependent manner in both LX-2 and HSC-T6 cells (Fig. 4A and B). To further confirm the role of these kinases in regulation of HSCs activation, MK2206 (MK), an Akt inhibitor, was recruited in the validation tests for LX-2 cells. MK treatment decreased Akt phosphorylation, which was associated with reduction of collagen I, α-SMA and TGF-β1 levels (Fig. 4C). Additionally, co-treatment of MK and PIN further enhanced the suppressing effect of PIN on HSCs activation (Fig. 4C). On the other hand, SC79 (SC), an Akt activator, enhanced Akt phosphorylation and the expressions of fibrotic markers in LX-2 cells, and partially abolished the effect of PIN at the concentration of 10 μM (Fig. 4D). The similar results were observed in the evaluation of extracellular TGF-β1 content of LX-2 cells (Fig. 4E), supporting that TGF-β production was translationally regulated by Akt with subsequent translation initiation factors.

We further investigated the total and phosphorylated Smad levels in LX-2 cells treated with MK and SC. As expected, the total and phosphorylated Smad levels were synergistically suppressed by PIN and MK (Fig. 4F), which indicated that PIN modulated Smad transcriptions through other pathways besides Akt. On the contrary, SC reversed PIN-induced suppression of total and phosphorylated Smad levels (Fig. 4G). Taken together, PIN suppressed the activation of HSCs, partially through inhibition of PI3K-Akt signaling pathway.

3.5. SIRT3-mediated ROS reduction was responsible for PIN regulation on ECMs

ROS were proposed to be crucial for the initiation and development of fibrosis (Ghatak et al., 2011; Richter et al., 2015). Indeed, PIN treatment significantly attenuated ROS accumulation in LX-2 cells in a dose-dependent manner, indicated by the fluorescent images (Fig. 5A) and flow cytometry analysis (Fig. 5B). SOD2 has been considered as one of the major antioxidants against ROS accumulation, and its activity was determined by SIRT3-mediated deacetylation (Qiu et al., 2010; Liu et al., 2017). Western blot analysis showed a slight increase of SOD2 protein, and a significant increase of SIRT3 level in LX-2 cells when treated with different concentrations of PIN (Fig. 5C). Similarly, SIRT3

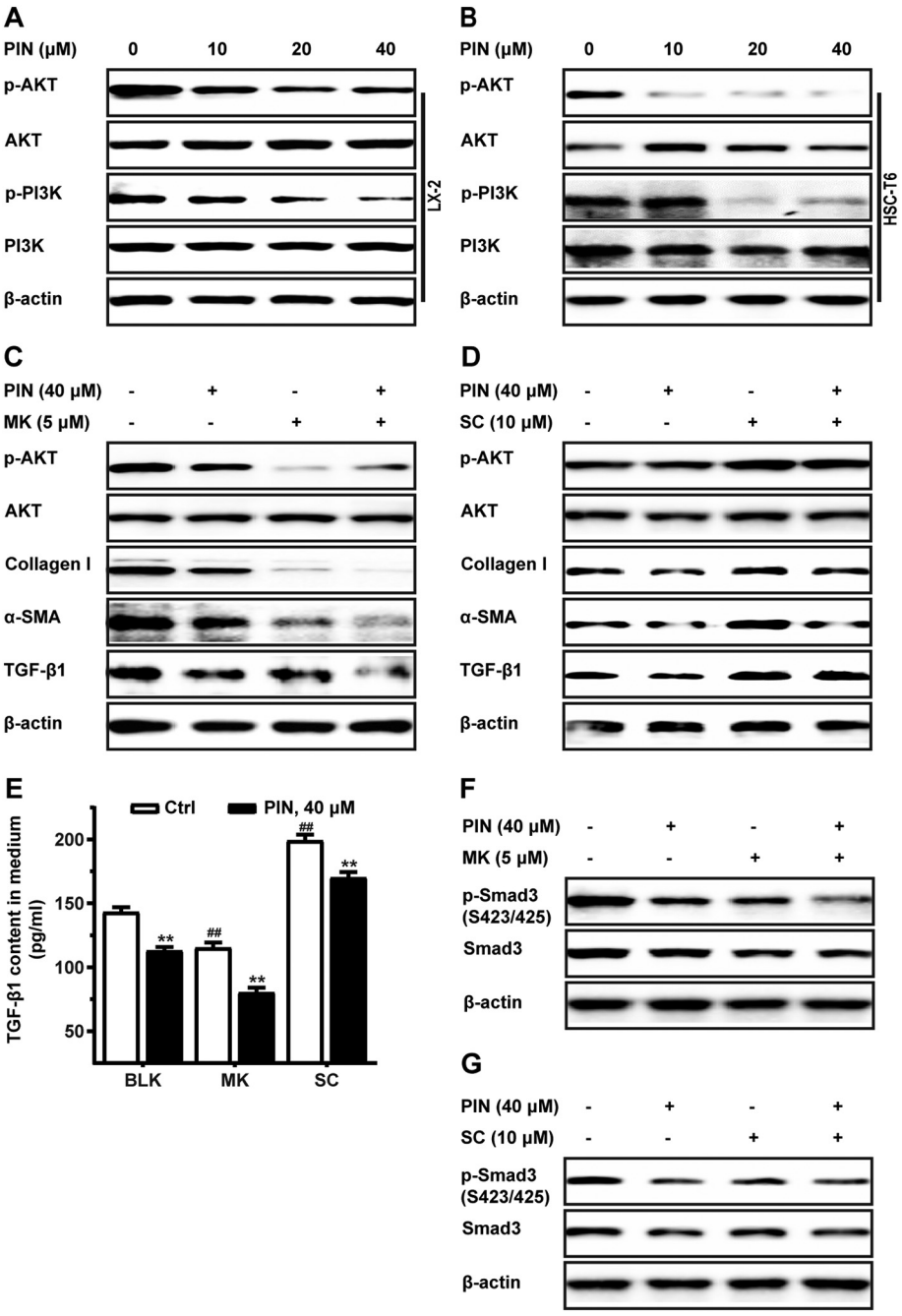

Fig. 4. PI3K-Akt signaling was involved in the anti-fibrotic effect of PIN. PIN inhibited Akt and PI3K phosphorylation in LX-2 (A) and HSC-T6 (B) cells. (C) PIN and Akt inhibitor MK synergistically decreased the fibrotic markers. (D) Akt activator SC partially reversed the effect of PIN on ECMs production. (E) Co-treatment of MK or SC with PIN affected the extracellular secretion of TGF-β1. (F) MK and PIN synergistically suppressed the expression of total and phosphorylated Smad3. (G) SC partly blocked the effect of PIN on total and phosphorylated Smad3 expressions. Measurements took $n = 6$ biological replicates. $^{**}p < 0.01$, PIN treated group *vs* control group; $^{\#\#}p < 0.01$, MK or SC treated group *vs* blank control group.

expression was elevated in PIN treated HSC-T6 cells (Fig. S2A). Meanwhile, the acetylated SOD2 was decreased in PIN-treated LX-2 cells in a dose-dependent manner (Fig. 5D), which indicated the activity of SOD2 was enhanced by PIN treatment.

To verify the role of SIRT3 in anti-fibrotic effect of PIN, *SIRT3* silenced LX-2 cell line (*S3KD*) was generated using shRNA targeting *SIRT3*. *S3KD* cells expressed around 60% less SIRT3 protein compared with that of the cells expressing scrambled shRNA (*SCR*) (Fig. 5E). SIRT3 silence resulted in remarkable increase of α-SMA expression compared with the *SCR* cells (Fig. 5E). The PIN-induced suppression of collagen I and α-SMA expressions was totally abolished in *S3KD* cells (Fig. 5E). Similarly, SIRT3 silence or treatment of SIRT3 inhibitor AGK induced more ROS accumulation, and totally reversed the ROS-alleviating effect of PIN (Figs. 5F and S2B). Taken together, PIN increased SIRT3 expression, which in turn deacetylated and activated SOD2 to enhance ROS clearance, resulting in inactivation of HSCs.

3.6. PIN activated GSK-3β to promote Smad degradation in hepatic stellate cells

Many studies reported different functions of diverse Smad phosphorylation sites, of which Ser423/425 appertained to the Mad Homology domains at the N-terminus (MH2) of Smad2/3 were encouragingly induced by TGF-β receptor 1 (TβR1) (Wrighton et al., 2009; Bruce and Sapkota, 2012); while, Thr66 in MH1 domain at the C-terminus of Smad2/3 was phosphorylated by activated GSK-3β and turned to degradation (Guo et al., 2008; Bruce and Sapkota, 2012; Lal et al., 2015). Hence, it was hypothesized that the decrease of total Smad in PIN treated cells might relate to GSK-3β mediated degradation of Smad protein. Western blot analysis showed the phosphorylated GSK-3β was decreased in LX-2 and HSC-T6 cells when treated with PIN in a dose-dependent manner (Figs. 6A and S2A). Most recently, SIRT3 was reported to directly deacetylate GSK-3β to prevent fibrosis (Sundaresan

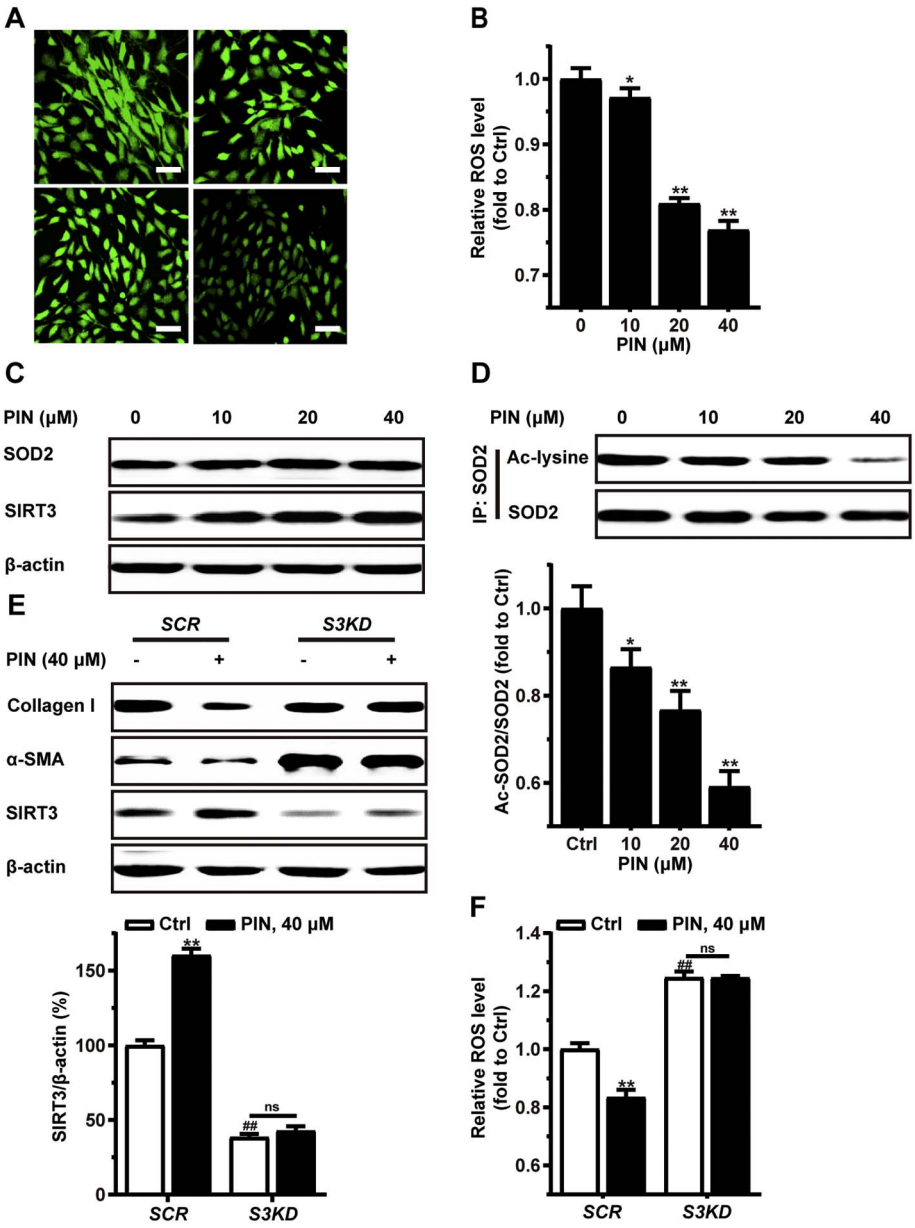

Fig. 5. SIRT3-mediated ROS reduction was responsible for anti-fibrotic effect of PIN. Intracellular ROS content was determined by fluorescent images (A) and flow cytometry (B). (C) SIRT3 expression was increased with the treatment of PIN. (D) PIN treatment reduced acetylated SOD2 level. (E) PIN suppressed ECM markers through SIRT3. (F) *SIRT3* knockdown totally blocked the ROS alleviating effect of PIN. Measurements took $n = 6$ biological replicates. $^{*}p < 0.05$ and $^{**}p < 0.01$, PIN treated group *vs* control group; $^{\#\#}p < 0.01$, *S3KD* group *vs SCR* group; ns, no significance. Scale bar = 50 μm.

et al., 2016). Thus, we subsequently investigated the acetylation level of GSK-3β in LX-2 cells. As expected, the IP experiments showed more SIRT3 was colocalized with GSK-3β and catalyzed the protein deacetylation (Fig. 6B).

To further verify the role of GSK-3β in Smad degradation, SB216763 (SB), an inhibitor GSK-3β, was recruited. As expected, SB suppressed the phosphorylation of GSK-3β, in turn to increase the total Smad level (Fig. 6C). Divergently, total Smad survived from diminishing when SB was present (Fig. 6C). Interestingly, treatment of SB partly reversed PIN induced Smad degradation. The above data suggested GSK-3β was activated in both phosphorylation and acetylation levels by PIN, to dually accelerate Smad degradation.

3.7. PIN suppressed hepatic stellate cells activation through a unified SIRT3-TGF-β-Smad signaling pathway

Previous study revealed SIRT3 blocked ROS-mediated hyperactivation of Akt signaling (Pillai et al., 2014). To confirm that PIN inhibited Akt activation *via* SIRT3, *S3KD* and *SCR* cells were treated with or without PIN. Western blot analysis indicated that SIRT3 silencing increased Akt phosphorylation, and totally blocked the suppressing effect of PIN on Akt phosphorylation (Fig. 7A). Consistently, Smad, along with TGF-β1 expression was increased in *S3KD* cells and LX-2 cells treated with AGK (Fig. 7B and Fig. S2C). The suppressing effect of PIN on the expression of TGF-β1 and Smad was totally abolished in *S3KD* cells and AGK treated LX-2 cells (Fig. 7B and Fig. S2C).

4. Discussion

P. chinense has been used for thousands of years to protect liver from alcoholic injury. Previous studies have disclosed *P. chinense* extracts possess protective effect against ethanol- or oxidant-induced liver injury (Cao et al., 2015; Hu et al., 2015; Wang et al., 2016). More than 30 compounds have been identified from this plant with anti-oxidative, anti-carcinomatous, and hypoglycemic effects (Wang et al., 2015). The current study further revealed the anti-fibrotic effect of *P. chinense in vitro*. Notably, PCE significantly suppressed ECM expressions in LX-2 cells but not in HSC-T6, which was likely due to the differences of the cell lines. Moreover, PIN was identified as the chemical principle responsible for the anti-fibrotic effect of *P. chinense*. PIN is a common

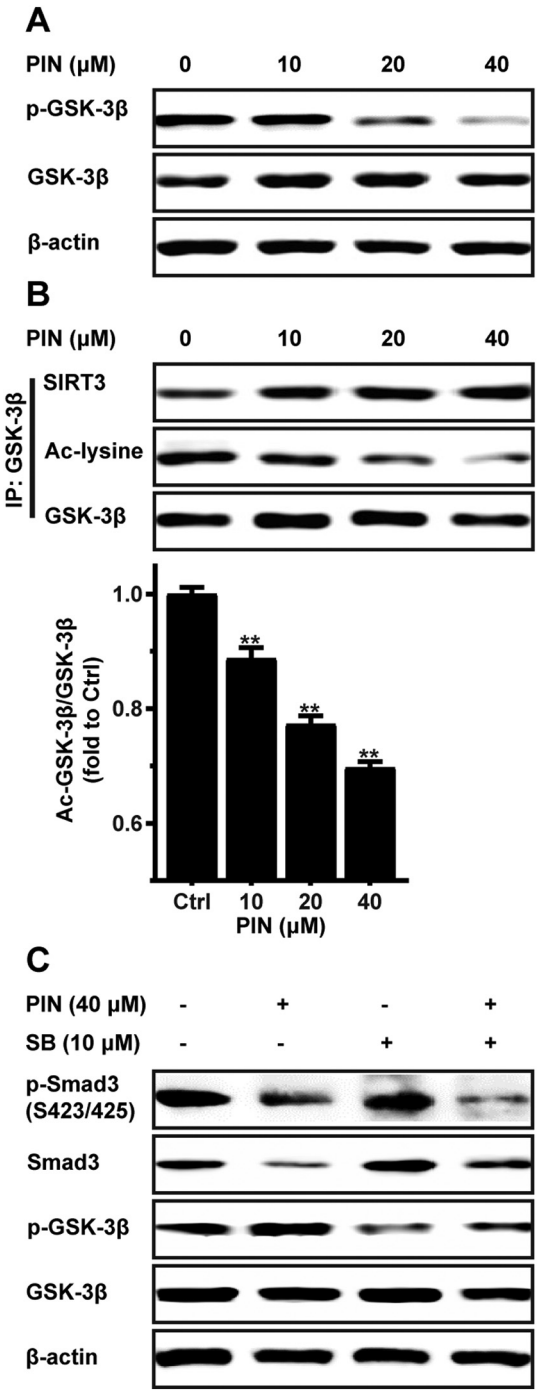

Fig. 6. PIN activated GSK-3β to promote Smad degradation in LX-2 cells. (A) PIN decreased phosphorylated GSK-3β expression. (B) the acetylated GSK-3β was reduced by PIN treatment. (C) SB blocked the effect of PIN of total Smad. Measurements took $n = 6$ biological implicates. $^{**}p < 0.01$, PIN treated group *vs* control group.

flavonoid widely existing in herbal medicines, which has been found with many pharmacological activities including vascular- and neuron-protective effects and anti-inflammatory activity (Gao et al., 2008; Gao et al., 2010; Soromou et al., 2012). Notwithstanding that PIN has been reported to serve as an anti-cirrhotic and anti-fibrotic component of propolis in distinct cell lines (Chen et al., 2008; Kao et al., 2013), the current study firstly demonstrated the treatment effect of hepatic fibrosis of PIN isolated from *P. chinense*.

To figure out the content of PIN in PCE, HPLC-UV analysis was conducted. Bewilderingly, the results showed that PIN was not the main constituent, and its content was about 0.1% in PCE (Fig. S3A), which implied that the potency of PIN could not fully represent that of PCE in suppressing HSCs activation. Although the content of PIN was low, PING and MPING, two PIN glucosides existed in PCE, was about 4.5% and 6.2%, respectively (Fig. S3A). Reports demonstrated that the anti-oxidation capacity of flavonoid glycosides was weaker than that of the corresponding flavonoid aglycones (Kim and Lee, 2004), which was in consistent with the anti-fibrotic results in the current study. The glycosides could be hydrolyzed to replenish PIN, which could partially explain the more potent anti-fibrotic effect of PCE. Additionally, KAE (3.7%) and KAE glycosides (5.9% for KAERP and 15.2% for KAEAF) are highly present in PCE (Fig. S3A), which also showed modest inhibitory effect on α-SMA expression. For the flavonoid aglycones QCT, KAE and PIN, it was reported that the hepatoprotective effect may be positively correlated to the number of phenolic hydroxyl groups in the B ring (Wang et al., 2016). However, the anti-fibrotic activity of such compounds was proved to be the opposite trends, which need further investigation on the underlying mechanisms. These flavonoids from PCE might show additional and/or synergetic effect with PIN. To explore the possible mechanisms of PCE and the incorporated chemical compositions to inhibit the activation of HSCs, protein analysis was performed. The results indicated that PCE suppressed HSCs activation through increasing SIRT3 expression, inhibiting AKT signaling, and enhancing GSK-3β activity (Fig. S3B), which was consistent with the transduction process demonstrated in PIN effect in the current study. These results well supported the synergetic effect of the chemical ingredients in PCE activity, and further suggested that the core active compositions could be the flavonoids containing a similar chemical structure. Moreover, it is possible that unidentified constituents in PCE with trace amount possess more potent anti-fibrotic effect. Therefore, further thoroughly chemical isolation is needed to fully elucidate the chemical principles of *P. chinense* for its anti-fibrotic effect.

Recent findings have demonstrated a concept of redox-fibrosis, suggesting that over accumulation of ROS is one of the key factors for fibrogenesis (Kurundkar and Thannickal, 2016; Torok, 2016). Many etiological factors could result in accumulation of ROS, which damage the cellular integrity and promote HSCs activation (Ghatak et al., 2011; Hsieh et al., 2011; Arellanes-Robledo et al., 2013). ROS contribute to fibrosis in the process of its initiation and evolution *via* different feed-forward and feedback loops (Kalogeris et al., 2014; Gorlach et al., 2015). Studies have shown that increased ROS is associated with TGF-β1 production (Richter et al., 2015). A perverse cycle was put forward in fibrotic diseases that TGF-β1 increased ROS production (Liu and Desai, 2015). Therefore, targeting on decreasing the excessive ROS accumulation is thought to be an effective therapeutic strategy for prevention and treatment of hepatic fibrosis. In the current study, PIN was found to attenuate ROS accumulation in LX-2 cells through elevating SIRT3 expression. It has been reported that increased SIRT3 expression resulted in the improvement of oxygen consumption rate in mitochondria and restriction of ROS synthesis, to further block Akt activation (Pillai et al., 2015). It was reported that Akt phosphorylation state was closely related to TGF-β1 promotion or inhibition, suggesting that Akt plays the role as a molecular switch for TGF-β1 induced osteoblastic differentiation (Suzuki et al., 2014). Our data showed PIN promoted the deacetylation of SOD2 through SIRT3, to enhance its activity and improve anti-oxidant capacity. Moreover, Akt phosphorylation was suppressed by PIN treatment as a result of the scarcity of hyperoxidation incited by ROS. Taken together, PIN prevented HSCs activation through SIRT3-SOD2-Akt-TGF-β1 pathway. At the current stage, we could not illustrate clearly how PIN regulates SIRT3 expression. It was reported that SIRT3 was activated by calorie restriction (Han and Someya, 2013) and exercise (Palacios et al., 2009), which is worthy to be further explored.

Existing evidences have manifested that TGF-β could be released as a result of inflammatory interactions, such as macrophages, or by structural cells such as airway epithelial cells, endothelial cells, and fibroblasts (Xiao et al., 2008; Kao et al., 2013). As the predominant

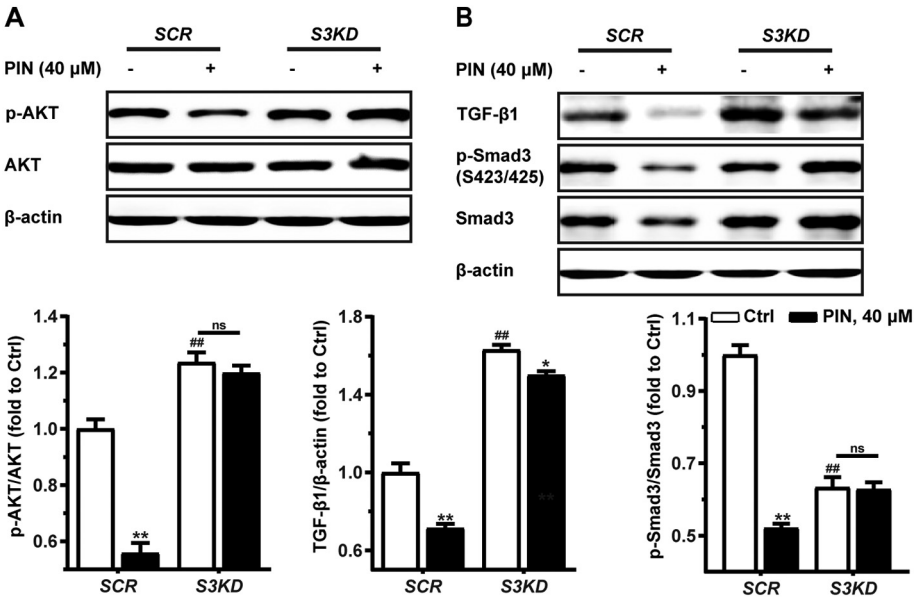

Fig. 7. PIN suppressed Akt phosphorylation and TGF-β-Smad pathway through SIRT3. (A) The suppressing effect of PIN on Akt phosphorylation was fully blocked by SIRT3 silence. (B) PIN regulated TGF-β-Smad signaling through SIRT3. Protein quantitative analysis for AKT phosphorylation (C), TGF-β1 expression (D) and Smad3 expression (E) in scrambled (*SCR*) and *SIRT3* knockdown (*S3KD*) LX-2 cells with or without 40 μM PIN treatment. Measurements took $n = 6$ biological replicates. $^{*}p < 0.05$ and $^{**}p < 0.01$, PIN treated group *vs* control group; $^{\#\#}p < 0.01$, *S3KD* group *vs SCR* group; ns, no significance.

pathogenic factor that drives fibrosis in various organs, TGF-β1 gathers multitudinous attention. Even though numerous evidences indicated that TGF-β1 could be the target for therapeutic strategies to inhibit tissue fibrosis, the adverse effects of adjusting this marker remained to be clarified (Kubiczkova et al., 2012; Meng et al., 2016). A study on phagocytes illustrated the production of TGF-β in response to apoptotic cells through phosphatidylserine recognition structures (PSRS), and identified the regulation of TGF-β production by inducing its transcription through activated mitogen-activating protein kinases (MAPKs) including p38, ERK, and JNK, or translation through Rho GTPase (RhoA), PI3K, Akt, and mammalian target of rapamycin (mTOR) with subsequent phosphorylation of translation initiation factor eukaryotic initiation factor 4E (eIF4E) (Xiao et al., 2008). Actually, we indeed observed the significant decrease of p38 MAPK and ERK phosphorylation in response to PIN treatment (Fig. S4), implying that TGF-β1 production was modulated by PIN through both transcriptional and translational processes.

Revocable phosphorylation of Smad plays a pivotal role in regulating its function (Bruce and Sapkota, 2012). r-Smads contain three structural features including two highly conserved MH1 and MH2, and a divergent linker region (LNK) (Massague et al., 2005; Bruce and Sapkota, 2012; Macias et al., 2015). Functionally, the MH2 domain is responsible for receptor interaction that allows heteromeric Smad complexes to be formatted (Macias et al., 2015). On the other hand, the MH1 domain negatively regulates the function of MH2 domain (Macias et al., 2015). In an ordinary TGF-β-Smad pathway, phosphorylation of the C-terminal Ser423/425 residues in MH2 domain by TβR1 drives the activation of r-Smads (Schmierer and Hill, 2007). In our study, PIN suppressed Smad3 phosphorylation at Ser423/425 residues. Surprisingly, we observed the consistent attenuation of both the C-terminal phosphorylated and total Smad proteins. Previous report indicated the SIRT3-mediated deacetylation and activation of GSK-3β blocked aging-associated tissue fibrosis in mice, and activated GSK-3β was a blocker of Smad (Sundaresan et al., 2016). Moreover, activated GSK-3β phosphorylated the Thr66 residue of Smad in the MH1 domain, resulted in the protein degradation (Guo et al., 2008). Currently, the phosphorylation and acetylation of GSK-3β were decreased through Akt and SIRT3, respectively, which promoted the kinase activity. Furthermore, abolishing GSK-3β arrested the subsidence of total Smad. The above results supported that PIN promoted Smad degradation, through SIRT3-GSK-3β pathway.

GSK-3 is a serine/threonine protein kinase that has been identified for over forty different proteins in a variety of different pathways (Lal et al., 2015). Involved in numerous central intracellular signaling pathways including cellular proliferation, migration, immune responses and apoptosis, GSK-3 was implicated in a number of diseases, for instance, fibrosis (Guo et al., 2017). Consistent with our findings, emerging evidence suggested that GSK-3β exerted its anti-fibrotic effect by directly interacting with Smad and negatively regulating the protein stability and enzymatic activity (Guo et al., 2008). In addition to the consensus that GSK-3β regulated TGF-β signaling pathway through phosphorylating Smad at the N-terminal to arouse its ubiquitination and degradation, recent study demonstrated the phosphorylation at Ser204 site in the LNK region by GSK-3β led to inhibition of Smad transcriptional activity (Bruce and Sapkota, 2012; Lal et al., 2015). In other words, through regulating the phosphorylation of Smad in both the MH1/2 and LNK domains, GSK-3β exerted dual control on TGF-β1-Smad signaling.

It is considered that activation of β-catenin dependent gene transcription leads to fibroblast activation and fibrosis in multiple organ systems (Yin et al., 2013; Affo et al., 2017; Sugimoto and Takei, 2017). GSK-3β is closely related to Wnt signal transduction pathway for the requirement of β-transduction repeat-containing protein (β-TrCP) to recognize the ubiquitination site of β-catenin (Gao et al., 2014). Adequate evidences illustrated that GSK-3β mediated phosphorylation of β-catenin resulted in the degradation and inactivation of the transcription factor which finally led to the remission of fibrosis (Arellanes-Robledo et al., 2013; Sundaresan et al., 2016; Guo et al., 2017). We observed that total β-catenin was decreased accompanied by the increase of β-catenin phosphorylation at Ser33/37 sites in PIN treated LX-2 cells (Fig. S5A), which indicated GSK-3β regulated β-catenin at Ser33/37 and subsequently caused the protein degradation. Bizarrely, β-catenin was likely accumulated in nucleus in PNT treated LX-2 cells (Figs. S5B and S5C), which seemed to be preposterous according to the consensus of GSK-3β interaction to β-catenin (Caspi et al., 2008). In fact, Akt was reported to phosphorylate β-catenin at Ser552 site, which took the responsibility of counterpoising its cytoplasmic accumulation and nuclear translocation (Fang et al., 2007). Nevertheless, distinct components involved in Wnt-β-catenin pathway reflected the effects on stability, localization and transcriptional activity of β-catenin (Gao et al., 2014). Taken together, we concluded that activated GSK-3β contributed relieve fibrotic symptoms through dual-controlling of TGF-β-Smad signaling and negatively regulated β-catenin activity. Squaring up to the facts of the multiple modification sites and the complexity of the

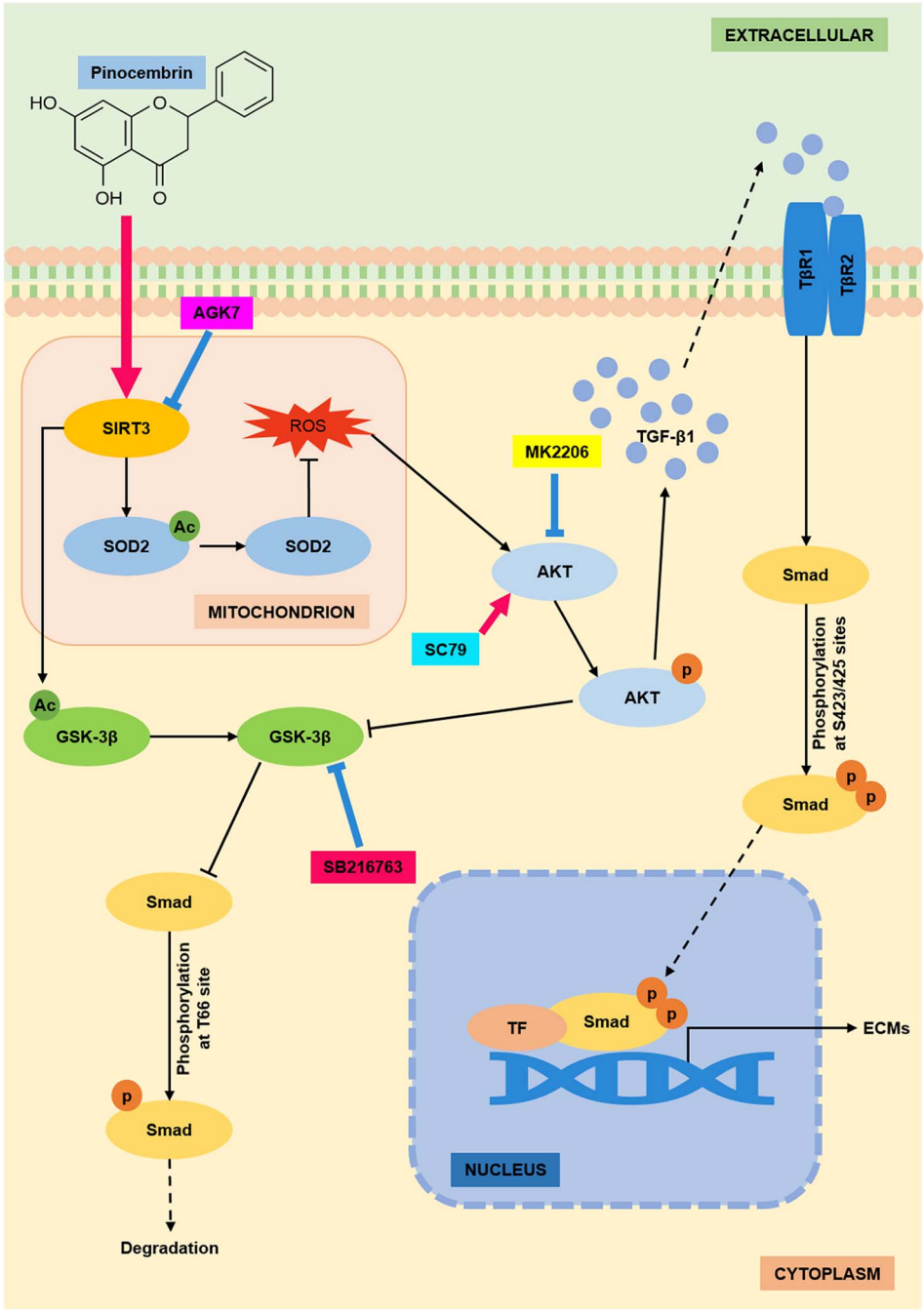

Fig. 8. PIN suppressed hepatic stellate cells activation through a unified SIRT3-TGF-β-Smad signaling pathway. PIN treatment elevated SIRT3 expression, followed with deacetylating and activating SOD2, to eliminate the accumulated ROS in mitochondria. Subsequently, Akt activity was inhibited and therefore TGF-β1 production and secretion was restricted, resulted in the inactivation and nuclear efflux of transcription factor Smad. Additionally, GSK-3β was activated through SIRT3 deacetylation, and inactivated Akt further enhanced GSK-3β effect. Thus, Smad was phosphorylated at N-terminal and turned to degradation. The dual-regulation of Smad effectively limited its transcriptional activity, decreased the production of ECMs, and suppressed HSCs activation.

influence given by the chemical, we consider that PIN was involved in other induction pathways and regulated β-catenin through some other mechanisms. Assuredly, the nuclear export of Smad took the more dominant position than the relocalization and activation of β-catenin in subsiding fibrotic symptoms in PIN treated LX-2 cells.

5. Conclusion

In conclusion, our study provides compelling evidences that the water extract of *P. chinense* remarkable suppresses the activation of HSCs. PIN, a flavonoid isolated from *P. chinense*, is verified to be the chemical principle. PIN inhibits ECM proteins expression through inactivating TGF-β-Smad signaling pathway. The expression and activity of SIRT3 is enhanced in PIN treated LX-2 and HSC-T6 cells, which in turn deacetylates and activates SOD2, attenuates ROS accumulation and suppresses Akt phosphorylation (Fig. 8). Moreover, PIN treatment diminishes the total Smad level through SIRT3-mediated activation of GSK-3β (Fig. 8). To the best of our knowledge, the current study firstly reports the anti-fibrotic activity of PIN and *P. chinense*. These results might provide a promising candidate for treatment of liver fibrosis.

Conflict of interest statement

The work described in this manuscript has not been published previously and is not under consideration for publication elsewhere. The submission and publication of this manuscript has been approved by all authors, and the authors declare no conflict of interest for the work in the manuscript.

Author contributions

FZ, AW and DL performed experiments. FZ and AW analyzed the

data. FZ drafted the manuscript. DL, YW and LL revised the manuscript. LL conceived and designed the study. All authors have approved the publication of manuscript.

Funding

This work was supported by the Research Fund of University of Macau (MYRG2015-00153-ICMS-QRCM and MYRG2017-00109-ICMS) and Science and Technology Development Fund, Macao S.A.R (FDCT 102/2017/A).

Acknowledgments

The authors thank Neautus Traditional Chinese Medicine Co. for supply of herbal material of *P. chinense*.

Appendix A. Supplementary data

Supplementary data to this article can be found online at https://doi.org/10.1016/j.taap.2018.01.009.

References

Affo, S., Yu, L.X., Schwabe, R.F., 2017. The role of cancer-associated fibroblasts and fibrosis in liver cancer. In: Abbas, A.K., Aster, J.C., Feany, M.B. (Eds.), Annual Review of Pathology: Mechanisms of Disease. Vol. 12. Annual Reviews, Palo Alto, pp. 153–186.

Arellanes-Robledo, J., Reyes-Gordillo, K., Shah, R., Dominguez-Rosales, J.A., Hernandez-Nazara, Z.H., Ramirez, F., Rojkind, M., Lakshman, M.R., 2013. Fibrogenic actions of acetaldehyde are beta-catenin dependent but wingless independent: a critical role of nucleoredoxin and reactive oxygen species in human hepatic stellate cells. Free Radic. Biol. Med. 65, 1487–1496.

Bruce, D.L., Sapkota, G.P., 2012. Phosphatases in SMAD regulation. FEBS Lett. 586, 1897–1905.

Cao, Y.W., Jiang, Y., Zhang, D.Y., Wang, M., Chen, W.S., Su, H.X., Wang, Y.T., Wan, J.B., 2015. Protective effects of *Penthorum chinense* Pursh against chronic ethanol-induced liver injury in mice. J. Ethnopharmacol. 161, 92–98.

Caspi, M., Zilberberg, A., Eldar-Finkelman, H., Rosin-Arbesfeld, R., 2008. Nuclear GSK-3 beta inhibits the canonical Wnt signalling pathway in a beta-catenin phosphorylation-independent manner. Oncogene 27, 3546–3555.

Chen, C.S., Wu, C.H., Lai, Y.C., Lee, W.S., Chen, H.M., Chen, R.J., Chen, L.C., Ho, Y.S., Wang, Y.J., 2008. NF-kappa B-activated tissue transglutaminase is involved in ethanol-induced hepatic injury and the possible role of propolis in preventing fibrogenesis. Toxicology 246, 148–157.

Fang, D.X., Hawke, D., Zheng, Y.H., Xia, Y., Meisenhelder, J., Nika, H., Mills, G.B., Kobayashi, R., Hunter, T., Lu, Z.M., 2007. Phosphorylation of beta-catenin by AKT promotes beta-catenin transcriptional activity. J. Biol. Chem. 282, 11221–11229.

Gao, M., Liu, R., Zhu, S.Y., Du, G.H., 2008. Acute neurovascular unit protective action of pinocembrin against permanent cerebral ischemia in rats. J. Asian Nat. Prod. Res. 10, 551–558.

Gao, M., Zhu, S.Y., Tan, C.B., Xu, B., Zhang, W.C., Du, G.H., 2010. Pinocembrin protects the neurovascular unit by reducing inflammation and extracellular proteolysis in MCAO rats. J. Asian Nat. Prod. Res. 12, 407–418.

Gao, C.X., Xiao, G.T., Hu, J., 2014. Regulation of Wnt/beta-catenin signaling by post-translational modifications. Cell Biosci. 4, 13.

Ghatak, S., Biswas, A., Dhali, G.K., Chowdhury, A., Boyer, J.L., Santra, A., 2011. Oxidative stress and hepatic stellate cell activation are key events in arsenic induced liver fibrosis in mice. Toxicol. Appl. Pharmacol. 251, 59–69.

Gorlach, A., Dimova, E.Y., Petry, A., Martinez-Ruiz, A., Hernansanz-Agustin, P., Rolo, A.P., Palmeira, C.M., Kietzmann, T., 2015. Reactive oxygen species, nutrition, hypoxia and diseases: problems solved? Redox Biol. 6, 372–385.

Guo, X., Ramirez, A., Waddell, D.S., Li, Z.Z., Liu, X.D., Wang, X.F., 2008. Axin and GSK3-beta control Smad3 protein stability and modulate TGF-beta signaling. Genes Dev. 22, 106–120.

Guo, Y.J., Gupte, M., Umbarkar, P., Singh, A.P., Sui, J.Y., Force, T., Lal, H., 2017. Entanglement of GSK-3 beta, beta-catenin and TGF-beta 1 signaling network to regulate myocardial fibrosis. J. Mol. Cell. Cardiol. 110, 109–120.

Han, C., Someya, S., 2013. Maintaining good hearing: calorie restriction, Sirt3, and glutathione. Exp. Gerontol. 48, 1091–1095.

Han, C.Y., Koo, J.H., Kim, S.H., Gardenghi, S., Rivella, S., Strnad, P., Hwang, S.J., Kim, S.G., 2016. Hepcidin inhibits Smad3 phosphorylation in hepatic stellate cells by impeding ferroportin-mediated regulation of Akt. Nat. Commun. 7, 13817.

He, Y.C., Peng, C., Xie, X.F., Chen, M.H., Li, X.N., Li, M.T., Zhou, Q.M., Guo, L., Xiong, L., 2015a. Penchinones A-D, two pairs of cis-trans isomers with rearranged neolignane carbon skeletons from *Penthorum chinense*. RSC Adv. 5, 76788 (Experimental gerontology 76794).

He, Y.C., Zou, Y., Peng, C., Liu, J.L., He, C.J., Guo, L., Xie, X.F., Xiong, L., 2015b. Penthorin A and B, two unusual 2,4′-epoxy-8,5′-neolignans from *Penthorum chinense*. Fitoterapia 100, 7–10.

Hebert, A.S., Dittenhafer-Reed, K.E., Yu, W., Bailey, D.J., Selen, E.S., Boersma, M.D., Carson, J.J., Tonelli, M., Balloon, A.J., Higbee, A.J., Westphall, M.S., Pagliarini, D.J., Prolla, T.A., Assadi-Porter, F., Roy, S., Denu, J.M., Coon, J.J., 2013. Calorie restriction and SIRT3 trigger global reprogramming of the mitochondrial protein acetylome. Mol. Cell 49, 186–199.

Hernandez-Gea, V., Friedman, S.L., 2011. Pathogenesis of liver fibrosis. In: Abbas, A.K., Galli, S.J., Howley, P.M. (Eds.), Annual Review of Pathology: Mechanisms of Disease. Vol 6. Annual Reviews, Palo Alto, pp. 425–456.

Hirschey, M.D., Shimazu, T., Goetzman, E., Jing, E., Schwer, B., Lombard, D.B., Grueter, C.A., Harris, C., Biddinger, S., Ilkayeva, O.R., Stevens, R.D., Li, Y., Saha, A.K., Ruderman, N.B., Bain, J.R., Newgard, C.B., Farese, R.V., Alt, F., Kahn, C.R., Verdin, E., 2010. SIRT3 regulates mitochondrial fatty-acid oxidation by reversible enzyme deacetylation. Nature 464, 121–137.

Houtkooper, R.H., Pirinen, E., Auwerx, J., 2012. Sirtuins as regulators of metabolism and healthspan. Nat. Rev. Mol. Cell Biol. 13, 225–238.

Hsieh, M.J., Hsieh, Y.S., Chen, T.Y., Chiou, H.L., 2011. Hepatitis C virus E2 protein induce reactive oxygen species (ROS)-related fibrogenesis in the HSC-T6 hepatic stellate cell line. J. Cell. Biochem. 112, 233–243.

Hu, Y.Y., Wang, S.P., Wang, A.Q., Lin, L.G., Chen, M.W., Wang, Y.T., 2015. Antioxidant and hepatoprotective effect of *Penthorum chinense* Pursh extract against *t*-BHP-induced liver damage in L02 cells. Molecules 20, 6443–6453.

Huang, D.D., Jiang, Y., Chen, W.S., Yao, F.Y., Sun, L.N., 2014. Polyphenols with antiproliferative activities from *Penthorum chinense* Pursh. Molecules 19, 11045–11055.

Huang, D.D., Jiang, Y., Chen, W.S., Yao, F.Y., Huang, G.H., Sun, L.N., 2015. Evaluation of hypoglycemic effects of polyphenols and extracts from *Penthorum chinense*. J. Ethnopharmacol. 163, 256–263.

Inagaki, Y., Okazaki, I., 2007. Emerging insights into transforming growth factor beta Smad signal in hepatic fibrogenesis. Gut 56, 284–292.

Kalogeris, T., Bao, Y.M., Korthuis, R.J., 2014. Mitochondrial reactive oxygen species: a double edged sword in ischemia/reperfusion vs preconditioning. Redox Biol. 2, 702–714.

Kao, H.F., Chang-Chien, P.W., Chang, W.T., Yeh, T.M., Wang, J.Y., 2013. Propolis inhibits TGF-beta 1-induced epithelial-mesenchymal transition in human alveolar epithelial cells via PPAR gamma activation. Int. Immunopharmacol. 15, 565–574.

Kim, D.O., Lee, C.Y., 2004. Comprehensive study an vitamin C equivalent antioxidant capacity (VCEAC) of various polyphenolics in scavenging a free radical and its structural relationship. Crit. Rev. Food Sci. Nutr. 44, 253–273.

Kubiczkova, L., Sedlarikova, L., Hajek, R., Sevcikova, S., 2012. TGF-beta - an excellent servant but a bad master. J. Transl. Med. 10, 183.

Kurundkar, A., Thannickal, V.J., 2016. Redox mechanisms in age-related lung fibrosis. Redox Biol. 9, 67–76.

Lal, H., Ahmad, F., Woodgett, J., Force, T., 2015. The GSK-3 family as therapeutic target for myocardial diseases. Circ.Res. 116, 138–149.

Liu, R.M., Desai, L.P., 2015. Reciprocal regulation of TGF-beta and reactive oxygen species: a perverse cycle for fibrosis. Redox Biol. 6, 565–577.

Liu, J.X., Li, D., Zhang, T., Tong, Q., Ye, R.D., Lin, L.G., 2017. SIRT3 protects hepatocytes from oxidative injury by enhancing ROS scavenging and mitochondrial integrity. Cell Death Dis. 8, e3158.

Lu, Q., Jiang, M.H., Jiang, J.G., Zhang, R.F., Zhang, M.W., 2012. Isolation and identification of compounds from *Penthorum chinense* Pursh with antioxidant and anti-hepatocarcinoma properties. J. Agric. Food Chem. 60, 11097–11103.

Macias, M.J., Martin-Malpartida, P., Massague, J., 2015. Structural determinants of Smad function in TGF-beta signaling. Trends Biochem.Sci. 40, 296–308.

Massague, J., 2012. TGF beta signalling in context. Nat. Rev. Mol. Cell Biol. 13, 616–630.

Massague, J., Seoane, J., Wotton, D., 2005. Smad transcription factors. Genes Dev. 19, 2783–2810.

Meng, X.M., Nikolic-Paterson, D.J., Lan, H.Y., 2016. TGF-beta: the master regulator of fibrosis. Nat. Rev. Nephrol. 12, 325–338.

Palacios, O.M., Carmona, J.J., Michan, S., Chen, K.Y., Manabe, Y., Ward, J.L., Goodyear, L.J., Tong, Q., 2009. Diet and exercise signals regulate SIRT3 and activate AMPK and PGC-1α in skeletal muscle. Aging 1, 771–783.

Pellicoro, A., Ramachandran, P., Iredale, J.P., Fallowfield, J.A., 2014. Liver fibrosis and repair: immune regulation of wound healing in a solid organ. Nat. Rev. Immunol. 14, 181–194.

Pillai, V.B., Sundaresan, N.R., Gupta, M.P., 2014. Regulation of Akt signaling by Sirtuins its implication in cardiac hypertrophy and aging. Circ.Res. 114, 368–378.

Pillai, V.B., Samant, S., Sundaresan, N.R., Raghuraman, H., Kim, G., Bonner, M.Y., Arbiser, J.L., Walker, D.I., Jones, D.P., Gius, D., Gupta, M.P., 2015. Honokiol blocks and reverses cardiac hypertrophy in mice by activating mitochondrial Sirt3. Nat. Commun. 6, 6656.

Puche, J.E., Saiman, Y., Friedman, S.L., 2013. Hepatic stellate cells and liver fibrosis. Compr. Physiol. 3, 1473–1492.

Qiu, X.L., Brown, K., Hirschey, M.D., Verdin, E., Chen, D., 2010. Calorie restriction reduces oxidative stress by SIRT3-mediated SOD2 activation. Cell Metab. 12, 662–667.

Reif, S., Lang, A., Lindquist, J.N., Yata, Y., Gabele, E., Scanga, A., Brenner, D.A., Rippe, R.A., 2003. The role of focal adhesion kinase-phosphatidylinositol 3-kinase-Akt signaling in hepatic stellate cell proliferation and type I collagen expression. J. Biol. Chem. 278, 8083–8090.

Remy, I., Montmarquette, A., Michnick, S.W., 2004. PKB/Akt modulates TGF-beta signalling through a direct interaction with Smad3. Nat. Cell Biol. 6, 358–365.

Richter, K., Konzack, A., Pihlajaniemi, T., Heljasvaara, R., Kietzmann, T., 2015. Redox-fibrosis: impact of TGF beta 1 on ROS generators, mediators and functional consequences. Redox Biol. 6, 344–352.

Schmierer, B., Hill, C.S., 2007. TGF beta-SMAD signal transduction: molecular specificity and functional flexibility. Nat. Rev. Mol. Cell Biol. 8, 970–982.

Shi, Z.D., Rockey, D.C., 2010. Interferon-gamma-mediated inhibition of serum response

factor-dependent smooth muscle-specific gene expression. J. Biol. Chem. 285, 32415–32424.
Someya, S., Yu, W., Hallows, W.C., Xu, J.Z., Vann, J.M., Leeuwenburgh, C., Tanokura, M., Denu, J.M., Prolla, T.A., 2010. Sirt3 mediates reduction of oxidative damage and prevention of age-related hearing loss under caloric restriction. Cell 143, 802–812.
Son, M.K., Ryu, Y.L., Jung, K.H., Lee, H., Lee, H.S., Yan, H.H., Park, H.J., Ryu, J.K., Suh, J.K., Hong, S., Hong, S.S., 2013. HS-173, a novel PI3K inhibitor, attenuates the activation of hepatic stellate cells in liver fibrosis. Sci. Rep. 3, 3470.
Soromou, L.W., Chu, X., Jiang, L.X., Wei, M.M., Huo, M.X., Chen, N., Guan, S., Yang, X.F., Chen, C.Z., Feng, H.H., Deng, X.M., 2012. *In vitro* and *in vivo* protection provided by pinocembrin against lipopolysaccharide-induced inflammatory responses. Int. Immunopharmacol. 14, 66–74.
Sugimoto, K., Takei, Y., 2017. Pathogenesis of alcoholic liver disease. Hepatol. Res. 47, 70–79.
Sundaresan, N.R., Bindu, S., Pillai, V.B., Samant, S., Pan, Y., Huang, J.Y., Gupta, M., Nagalingam, R.S., Wolfgeher, D., Verdin, E., Gupta, M.P., 2016. SIRT3 blocks aging-associated tissue fibrosis in mice by deacetylating and activating glycogen synthase kinase 3 beta. Mol. Cell. Biol. 36, 678–692.
Suzuki, E., Ochiai-Shino, H., Aoki, H., Onodera, S., Saito, A., Saito, A., Azuma, T., 2014. Akt activation is required for TGF-beta 1-induced osteoblast differentiation of MC3T3-E1 pre-osteoblasts. PLoS One 9, e112566.
Torok, N.J., 2016. Dysregulation of redox pathways in liver fibrosis. Am. J. Physiol.-Gastroint. Liver Physiol. 311, G667–G674.
Troeger, J.S., Mederacke, I., Gwak, G.Y., Dapito, D.H., Mu, X.R., Hsu, C.C., Pradere, J.P., Friedman, R.A., Schwabe, R.F., 2012. Deactivation of hepatic stellate cells during liver fibrosis resolution in mice. Gastroenterology 143, 1073–1083.
Wang, F.P., Li, L., Li, J., Wang, J.Y., Wang, L.Y., Jiang, W., 2013. High mobility group box-1 promotes the proliferation and migration of hepatic stellate cells via TLR4-dependent signal pathways of PI3K/Akt and JNK. PLoS One 8, e64373.
Wang, M., Jiang, Y., Liu, H.L., Chen, X.Q., Wu, X., Zhang, D.Y., 2014. A new flavanone from the aerial parts of *Penthorum chinense*. Nat. Prod. Res. 28, 70–73.
Wang, A.Q., Lin, L.G., Wang, Y.T., 2015. Traditional Chinese herbal medicine *Penthorum chinense* Pursh: a phytochemical and pharmacological review. Am. J. Chin. Med. 43, 601–620.
Wang, A.Q., Wang, S.P., Jiang, Y., Chen, M.W., Wang, Y.T., Lin, L.G., 2016. Bio-assay guided identification of hepatoprotective polyphenols from *Penthorum chinense* Pursh on *t*-BHP induced oxidative stress injured L02 cells. Food Funct. 7, 2074–2083.
Wrighton, K.H., Lin, X., Feng, X.H., 2009. Phospho-control of TGF-beta superfamily signaling. Cell Res. 19, 8–20.
Xiao, Y.Q., Freire-de-Lima, C.G., Schiemann, W.P., Bratton, D.L., Vandivier, R.W., Henson, P.M., 2008. Transcriptional and translational regulation of TGF-beta production in response to apoptotic cells. J. Immunol. 181, 3575–3585.
Yin, C.Y., Evason, K.J., Asahina, K., Stainier, D.Y.R., 2013. Hepatic stellate cells in liver development, regeneration, and cancer. J. Clin. Invest. 123, 1902–1910.
Yu, W., Dittenhafer-Reed, K.E., Denu, J.M., 2012. SIRT3 protein deacetylates isocitrate dehydrogenase 2 (IDH2) and regulates mitochondrial redox status. J. Biol. Chem. 287, 14078–14086.
Zeng, Q.H., Zhang, X.W., Xu, X.L., Jiang, M.H., Xu, K.P., Piao, J.H., Zhu, L., Chen, J., Jiang, J.G., 2013. Antioxidant and anticomplement functions of flavonoids extracted from P*enthorum chinense* Pursh. Food Funct. 4, 1811–1818.
Zhang, Y.E., 2009. Non-Smad pathways in TGF-beta signaling. Cell Res. 19, 128–139.
Zhang, L., Zhou, F.F., ten Dijke, P., 2013. Signaling interplay between transforming growth factor-beta receptor and PI3K/AKT pathways in cancer. Trends Biochem.Sci. 38, 612–620.